1872 *Inorg. Chem.* **2010**, *49*, 1872–1883
DOI: 10.1021/ic902265e

Inorganic Chemistry
Article

Design and Synthesis of Sn-Porphyrin Based Molecular Gates

Aurélie Guenet, Ernest Graf, Nathalie Kyritsakas, and Mir Wais Hosseini*

Laboratoire de Chimie de Coordination Organique (UMR-CNRS 7140), Université de Strasbourg, Institut Le Bel, 4 rue Blaise Pascal, 67000 Strasbourg, France

Received November 16, 2009

The design, synthesis, and structural characterization, both in solution by ^{1}H NMR and in the solid state by X-ray diffraction on single crystals, of a series of molecular gates based on Sn-porphyrin derivatives are presented. The molecular system is based on a porphyrin core bearing at the *meso* positions either phenyl or pyridyl groups as a stator, octahedral Sn(IV) cation located at the center of the porphyrin as a hinge, and different handles connected to the porphyrin through Sn−O axial bonds. The stability of the complexes in the presence of different acids is also reported.

Introduction

A molecular motor may be defined as a molecular architecture for which a movement may be induced by external stimuli. The induced and controlled movement must take place between a fixed and a mobile portion. In principle, one may envisage either translational or rotational motors.[1−28] Movement plays a fundamental role in the living world.[2] Biological motors of the linear type based on myosine[3,4] or kinesine[5,6] have been discovered and studied. A rotary motor based on ATPase has been also described.[7,8] Dealing with abiotic systems, the two pioneer investigations undertaken by

*To whom correspondence should be addressed. E-mail: hosseini@unistra.fr. Phone: 33 368851323. Fax: 33 368851325.

(1) Launay, J.-P. *Actual. Chim.* **2001**, 33–38.
(2) Howard, J. *Nature* **1997**, *389*, 561–567.
(3) Finer, J. T.; Simmons, R. M.; Spudich, J. A. *Nature* **1994**, *368*, 113–119.
(4) Whittaker, M.; Wilson-Kubalek, E. M.; Smith, J. E.; Faust, L.; Milligan, R. A.; Sweeney, H. L. *Nature* **1995**, *378*, 748–751.
(5) Sablin, E. P.; Kull, F. J.; Cooke, R.; Vale, R. D.; Fletterick, R. J. *Nature* **1996**, *380*, 555–559.
(6) Meyhöfer, E.; Howard, J. *Proc. Natl. Acad. Sci. U.S.A.* **1995**, *92*, 574–578.
(7) Elston, T.; Wang, H. Y.; Oster, G. *Nature* **1998**, *391*, 510–513.
(8) Noji, H.; Yasuda, R.; Yoshida, M.; Kinosita, K., Jr. *Nature* **1997**, *386*, 299–302.
(9) (a) Balzani, V.; Gomez-Lopez, M.; Stoddart, J. F. *Acc. Chem. Res.* **1998**, *31*, 405–414. (b) Stoddart, J. F. *Acc. Chem. Res.* **2001**, *34*, 410–411.
(10) (a) Sauvage, J.-P. *Science* **2001**, *291*, 2105–2106. (b) Sauvage, J. P. *Acc. Chem. Res.* **1998**, *31*, 611–619. (c) Sauvage, J.-P. *Actual. Chim.* **2003**, 119–125. (d) Collin, J.-P.; Kern, J.-M.; Raehm, L.; Sauvage, J.-P. In *Molecular Switches*; Feringa, B. L., Ed.; Wiley-VCH Verlag GmbH: Weinheim, Germany, 2001; pp 249−280.
(11) Kelly, T. R.; De Silva, H.; Silva, R. A. *Nature* **1999**, *401*, 150–152.
(12) (a) Koumura, N.; Zijlstra, R. W. J.; van Delden, R. A.; Harada, N.; Feringa, B. L. *Nature* **1999**, *401*, 152–155. (b) Ter Wiel, M. K. J.; van Delden, R. A.; Meetsma, A.; Feringa, B. L. *J. Am. Chem. Soc.* **2005**, *127*, 14208–14222. (c) van Delden, R. A; ter Wiel, M. K. J.; Koumura, N.; Feringa, B. L. In *Molecular Motors*; Schliwa, M., Ed.; Wiley-VCH Verlag GmbH & Co. KGaA: Weinheim, Germany, 2003; pp 559−577.
(13) (a) Morin, J. F.; Shirai, Y.; Tour, J. M. *Org. Lett.* **2006**, *8*, 1713–1716. (b) Shirai, Y.; Osgood, A. J.; Zhao, Y.; Yao, Y.; Saudan, L.; Yang, H.; Yu-Hung, C.; Alemany, L. B.; Sasaki, T.; Morin, J.-F.; Guerrero, J. M.; Kelly, K. F.; Tour, J. M. *J. Am. Chem. Soc.* **2006**, *128*, 4854–4864.
(14) (a) Chiaravalloti, F.; Gross, L.; Rieder, K.-H.; Stojkovic, S. M.; Gourdon, A.; Joachim, C.; Moresco, F. *Nat. Mater.* **2007**, *6*, 30–33. (b) Grill, L.; Rieder, K.-H.; Moresco, F.; Jimenez-Bueno, G.; Wang, C.; Rapenne, G.; Joachim, C. *Surf. Sci.* **2005**, *584*, L153–L158.
(15) Carella, A.; Jaud, J.; Rapenne, G.; Launay, J.-P. *Chem. Commun.* **2003**, 2434–2435.
(16) Balzani, V.; Credi, A.; Raymo, F. M.; Stoddart, J. F. *Angew. Chem., Int. Ed.* **2000**, *39*, 3348–3391.
(17) *Molecular Machines and Motors*; Sauvage, J.-P., Ed.; Structure & Bonding; Springer: Berlin, Heidelberg, 2001; Vol. *99*.
(18) *Molecular Switches*; Feringa, B. L., Ed.; Wiley-VCH Verlag GmbH: Weinheim, Germany, 2001.
(19) Balzani, V.; Venturi, M.; Credi, A. *Molecular devices and machines: a journey into the nanoworld*; Wiley-VCH Verlag GmbH: Weinheim, Germany, 2003.
(20) (a) Collin, J.-P.; Dietrich-Buchecker, C.; Gavina, P.; Jimenez-Molero, M. C.; Sauvage, J.-P. *Acc. Chem. Res.* **2001**, *34*, 477–487. (b) Jiménez, M. C.; Dietrich-Buchecker, C.; Sauvage, J.-P. *Angew. Chem., Int. Ed.* **2000**, *39*, 3284–3287. (c) Jimenez-Molero, M. C.; Dietrich-Buchecker, C.; Sauvage, J.-P. *Chem.—Eur. J.* **2002**, *8*, 1456–1466.
(21) Ballardini, R.; Balzani, V.; Credi, A.; Gandolfi, M. T.; Venturi, M. *Acc. Chem. Res.* **2001**, *34*, 445–455.
(22) (a) Feringa, B. L. *Acc. Chem. Res.* **2001**, *34*, 504–513. (b) Eelkema, R.; Pollard, M. M.; Vicario, J.; Katsonis, N.; Ramon, B. S.; Bastiaansen, C. W. M.; Broer, D. J.; Feringa, B. L. *Nature* **2006**, *440*, 163–163.
(23) Schalley, C. A.; Beizai, K.; Vögtle, F. *Acc. Chem. Res.* **2001**, *34*, 465–476.
(24) (a) Kelly, T. R. *Acc. Chem. Res.* **2001**, *34*, 514–522. (b) Kelly, T. R.; Cai, X.; Damkaci, F.; Panicker, S. B.; Tu, B.; Bushell, S. M.; Cornella, I.; Piggott, M. J.; Salives, R.; Cavero, M.; Zhao, Y.; Jasmin, S. *J. Am. Chem. Soc.* **2007**, *129*, 376–386.
(25) Harada, A. *Acc. Chem. Res.* **2001**, *34*, 456–464.
(26) Shinkai, S.; Ikeda, M.; Sugasaki, A.; Takeuchi, M. *Acc. Chem. Res.* **2001**, *34*, 494–503.
(27) Amendola, V.; Fabbrizzi, L.; Mangano, C.; Pallavicini, P. *Acc. Chem. Res.* **2001**, *34*, 488–493.
(28) (a) Flood, A. H.; Ramirez, R. J. A.; Deng, W.-Q.; Muller, R. P.; Goddard, W. A., III; Stoddart, J. F. *Aust. J. Chem.* **2004**, *57*, 301–322. (b) Liu, Y.; Flood, A. H.; Bonvallet, P. A.; Vignon, S. A.; Northrop, B. H.; Tseng, H. R.; Jeppesen, J. O.; Huang, T. J.; Brough, B.; Baller, M.; Magonov, S.; Solares, S. D.; Goddard, W. A.; Ho, C. M.; Stoddart, J. F. *J. Am. Chem. Soc.* **2005**, *127*, 9745–9759.

Published on Web 01/22/2010

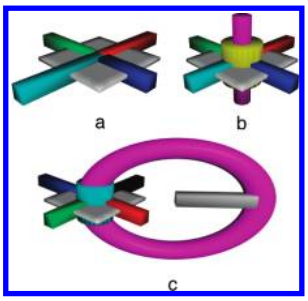

Figure 1. Schematic representation of three parts of a rotary motor: stator (a), hinge complexed by the stator (b), and the rotor (c).

the groups of Stoddart-Balzani and by Sauvage and co-workers must be quoted. In the case of Stoddart, following the supramolecular approach, translational molecular motors based on the use of only organic moieties arranged in rotaxane type structures have been described.[9] On the other hand, Sauvage and collaborators, using coordination chemistry, described rotational motors based on induced changes in the coordination number and geometry around metal centers in catenane type architectures.[10] The same group has also reported a translational motor based on rotaxanes bearing a redox active metal center. On the basis of the same type of strategy, Sauvage and co-workers have also reported an artificial mobile system qualified as a molecular muscle.[20] Recently two other pertinent reports described molecular motors based on thermal (Kelly et al.)[11] or photochemical (Feringa et al.)[12] processes. Other types of molecular machines undergoing movement on surfaces such as cars,[13] wheelbarrows,[14] and turnstiles[15] have been also investigated.

Design of molecular machines still remains a challenging task and continues to attract attention.[16−32] For the design of abiotic motors, four features must be taken into account: (i) the amplitude of the movement, (ii) the speed of the movement, (iii) the directionality of the movement, and (iv) the reversibility of the process. These aspects are essential and need further studies. A possible design of a rotary molecular motor may be based on a three-part system (Figure 1): a stator (a), a porphyrin bearing up to 4 peripheral coordination sites, a hinge (b), hypervalent Sn(IV) octahedral center complexed by the tetraaza core of the porphyrin, and a rotor (c), a molecular fragment, doubly attached to the hinge, bearing a mono dentate coordination site oriented toward the porphyrin backbone.

The viability of the approach, previously reported in a communication,[33] was demonstrated on a molecular gate. The design of the latter is based on a stator bearing a single coordination site oriented divergently from its center, a hinge allowing to connect the handle, and a rotatable handle equipped with a monodentate coordination site oriented toward the hinge (Figure 2). In the absence of a metal ion, the handle rotates freely about the hinge (open gate) whereas in its presence, the gate is locked by binding of the metal by both coordinating sites (closed gate). The action of the metal

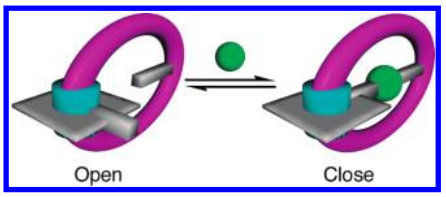

Figure 2. Schematic representation of a molecular gate based on a hinge (gray square) and a handle (purple unit) bearing each one recognition site. Opening and closing motions of the gate are induced by coordination of a metal ion (green sphere) to the two recognition sites. The handle is considered as the rotor and the hinge as the stator.

ion may be regarded as an external stimulus responsible for the locking of the motion.

Herein, we report on our complete investigation dealing with the design, synthesis, and structural investigations of molecular gates based on the above-mentioned design principles.

Results and Discussion

Design of the System. As stated above, the gate consists of three main parts: a stator, a hinge, and a handle. The stator is based on a porphyrin unit, the latter being the candidate of choice since its *meso* positions can be substituted as desired.[34] For the present study, the porphyrin backbone was equipped with three phenyl groups and one pyridine moiety as a monodentate coordinating site (compounds **1** and **2**). To impose outward orientation of the coordinating site, the pyridine moiety was connected to the porphyrin core at position 4. For comparison purposes, compounds **3** and **4**, analogues of **1** and **2**, respectively, were prepared. Compound **3** is based on the same handle as **1**; however it does not contain a coordinating site on the stator and thus its rotation should not be altered by the presence of the metal cation. Compound **4** is an analogue of **3**, but the handle was shortened by two glycol units allowing thus to study the role played by the length of the handle. Compound **5**, which contains a coordination site located on the stator and an oligoethyleneglycol fragment as the handle was also prepared. Finally, compound **6** bearing no coordination site was synthesized. As for the hinge, Sn(IV), a strong oxophilic Lewis acid adopting an octahedral coordination geometry, was chosen.[35] Indeed, its binding to the tetrapyrrolic core of the porphyrin leads to a stable dicationic metallaporphyrin offering two apical positions in *trans* configuration for the connection of the handle. Furthermore, the introduction of the handle through the formation of two Sn−O bonds leads to a neutral complex. Finally, the handle was designed as a relatively flexible bis-monodentate ligand possessing one central recognition site (pyridine) and two terminal coordinating sites of the phenate type (resorcinol moiety) allowing to connect the handle and the hinge together. The pyridine and resorcinol units are connected via spacers with variable length.

The purpose of this study was essentially 3-fold: (1) verify the coordination mode of the handle to the tin porphyrin, (2) determine the appropriate size of the

(29) Kinbara, K.; Aida, T. *Chem. Rev.* **2005**, *105*, 1377–1400.
(30) *Molecular machines*; Kelly, T. R., Ed.; Topics in Current Chemistry; Springer: Berlin, Heidelberg, 2005; Vol. *262*.
(31) Browne, W. R.; Feringa, B. L. *Nat. Nanotechnol.* **2006**, *1*, 25–35.
(32) Kay, E. R.; Leigh, D. A.; Zerbetto, F. *Angew. Chem., Int. Ed.* **2007**, *46*, 72–191.
(33) Guenet, A.; Graf, E.; Kyritsakas, N.; Allouche, L.; Hosseini, M. W. *Chem. Commun.* **2007**, 2935–2937.
(34) (a) Lindsey, J. In *The Porphyrin Handbook*; Kadish, K. M., Smith, K. M., Guilard, R., Eds.; Academic Press: San Diego, CA, 2000; Vol. *1*, pp 45−118; (b) Lindsey, J. S. *Acc. Chem. Res.* **2009**, DOI: 10.1021/ar900212t.
(35) Arnold, D. P.; Blok, J. *Coord. Chem. Rev.* **2004**, *248*, 299–319.

Scheme 1. Structures of Compounds **1**−**6** and Labelling of Hydrogen Atoms

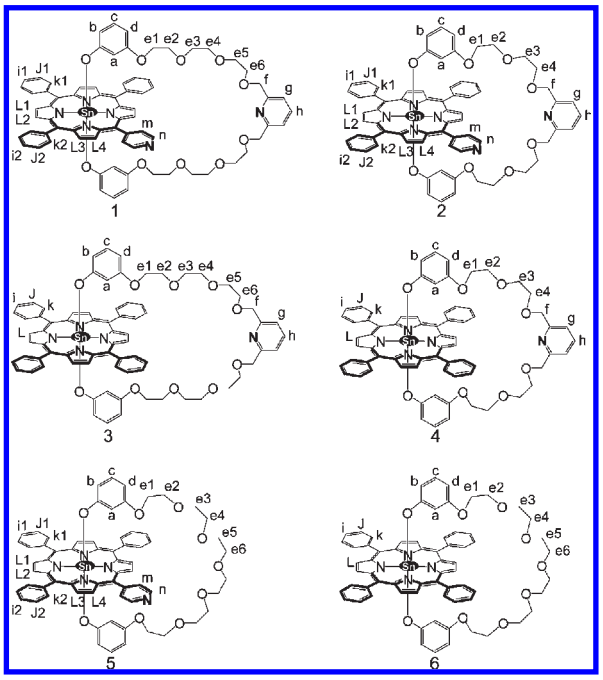

Scheme 2

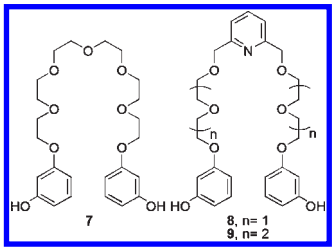

handle by varying the length of the spacer, and (3) find appropriate stimuli to open and close the gate. Indeed, free rotation of the handle around the hinge in the absence of a stimulus is one of the prerequisites for the gate. To tune these parameters, different prototypes of the gate were prepared.

The first prototype (compound **6**, Scheme 1), based on hexaethyleneglycol as the handle bearing at its two extremities a resorcinol moiety **7** (Scheme 2), possesses no specific coordination sites neither on the stator nor on the handle. This compound was prepared to determine the actual coordination mode of the bis-monodentate handle to the tin atom (formation of discrete complex vs polymeric entities) and furthermore to demonstrate that the rotation of the handle around the stator is not altered by the presence of the metal. For the second type of prototypes, either the handle (compound **3** and **4**, Scheme 1) or the stator (compound **5**, Scheme 1) is equipped with a pyridine as coordinating site. To determine the appropriate length of the two oligoethyleneglycol fragments connecting the pyridine moiety to resorcinol groups, based on Corey−Pauling−Koltun (CPK) models, two handles differing only by the length of the spacer were prepared (compounds **8** and **9**, Scheme 2).

Synthesis of Handles. The synthesis of **7** was achieved in five steps (Scheme 3). Starting with the monoprotected resorcinol **10**, its reaction, under acidic conditions, with

Scheme 3[a]

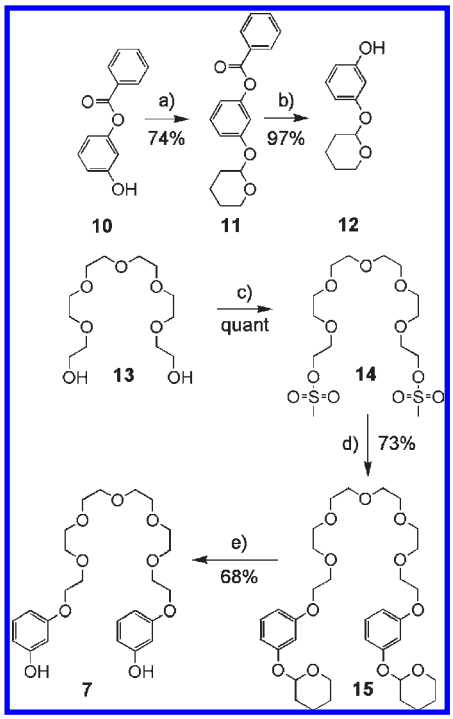

[a] Reagents and conditions: (a) DHP, TFA, EtOAc, RT; (b) 1.5 M $NaOH_{aq}$, THF, RT; (c) CH_3SO_2Cl, Et_3N, THF, RT; (d) **12**, NaH, THF, reflux; (e) HCl_{aq}, MeOH, RT.

dihydropyran in dry EtOAc gave **11** in 74% yield. The hydrolysis of the latter by NaOH in a mixture of tetrahydrofuran (THF)/H_2O afforded the compound **12** in 97% yield. It is worth noting that the direct protection of resorcinol with DHP[36] was found to be less efficient (lower yields) and required a more tedious purification step. The second starting material, compound **13**, was activated into its dimesylate derivative **14** in quantitative yield upon reaction with methanesulfonyl chloride at room temperature (RT) in THF and in the presence of triethylamine. The reaction of **12** with **14** in the presence of sodium hydride in refluxing THF during 2 days afforded the pure compound **15** in 73% yield. Finally, the deprotection of **15** under acidic conditions in methanol at RT afforded the desired compound **7** in 68% yield.

Because of the introduction of the pyridine moiety, the synthesis of the other two handles **8** and **9** required three more synthetic steps (Scheme 4). Starting with 2,6-bis-(hydroxymethyl)pyridine **16**, its dichlorination by thionyl chloride in dry THF[37] afforded the compound **17** in 88% yield. On the other hand, starting either with **18** or **19**, their monoprotection by the THP group affording compounds **20** or **21** was achieved in 42% and 50% yields, respectively, upon treatment at RT with dihydropyran in dry chloroform and in the presence of pyridinium tosylate.[38] It should be noted that, since the monoprotected oligoethyleneglycols **20** and **21** are less volatile than the diprotected derivatives, no chromatography was required

(36) Brown, P. E.; Lewis, R. A.; Waring, M. A. *J. Chem. Soc., Perkin Trans. 1* **1990**, 2979–2988.
(37) Rezzonico, B.; Grigon-Dubois, M. J. *J. Chem. Res.* (*S*) **1994**, 142–143.
(38) Acerete, C.; Bueno, J. M.; Campayo, L.; Navarro, P.; Rodriguez-Franco, M. I. *Tetrahedron* **1994**, *50*, 4765–4774.

Scheme 4[a]

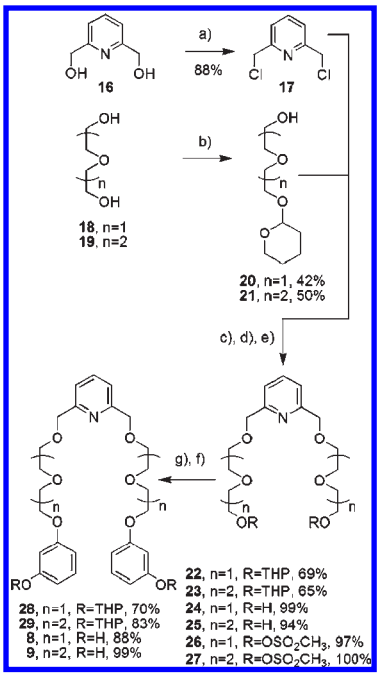

[a] Reagents and conditions: (a) $SOCl_2$, THF, reflux; (b) DHP, PPTS, $CHCl_3$, RT; (c) NaH, THF, reflux; (d) HCl_{aq}, MeOH, RT; (e) $ClSO_2CH_3$, Et_3N, THF, RT; (f) **12**, NaH, THF, reflux; (g) HCl_{aq}, MeOH.

and simple drying of the crude mixture for 24 h under vacuum gave the desired compounds in high yields and large amounts.

Following a reported procedure,[39] upon refluxing for 5 days a mixture of either **20** or **21** with **17** and sodium hydride in dry THF, the functionalized pyridine derivatives **22** and **23** were obtained in 69 and 65% yield, respectively. Their deprotection affording the diol derivatives **24** and **25** was achieved in 99% and 94% yield, respectively, by treatment with a mixture of methanol/aqueous HCl at RT. The activation of diols **24** and **25** into their dimesylate derivatives, **26** and **27** respectively, was achieved by treatment at RT with methanesulfonyl chloride in the presence of triethylamine in dry THF. The introduction of the resorcinol moiety leading to compounds **28** and **29** was done in 70% and 83% yield, respectively, by reaction of either **26** or **27** with the monoprotected resorcinol derivative **12** (Scheme 3) under reflux for 3 days in dry THF and in the presence of NaH. Finally, the desired compounds **8** and **9** were obtained in 88% and 99% yields, respectively, upon treatment at RT of **28** or **29** with methanol/aqueous HCl.

Synthesis of Porphyrins. The two porphyrins considered as stators were the *meso*-substituted derivatives **30** and **31** (Scheme 5). Whereas compound **30** bears four phenyl groups at the *meso* positions, porphyrin **31** is equipped with a pyridine unit which should act as a peripheral coordinating site. Following the method described by Adler et al.,[40] the *meso*-tetraphenylporphyrin **30** was prepared in 24% yield upon condensation of

Scheme 5. Structures of Compounds **30**−**34**

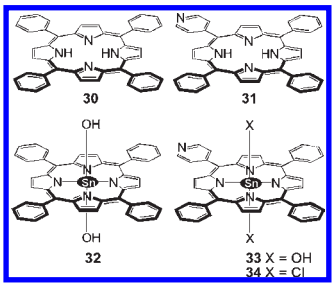

Scheme 6. Structures of Compounds **35** and **36** and Labelling of Hydrogen Atoms

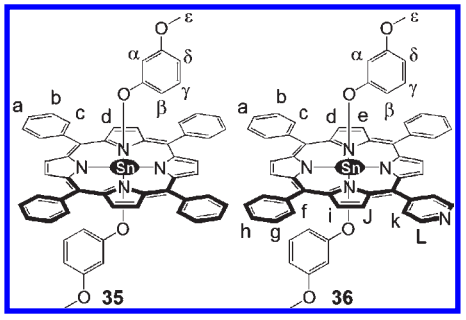

pyrrole with benzaldehyde in refluxing propionic acid under aerobic conditions. Compound **31** was obtained in 5% yield after chromatography, as previously described[41] by mixing benzaldehyde, 4-pyridinecarboxaldehyde, and pyrrole in refluxing propionic acid.

Synthesis of Tin Porphyrins. As stated above, the stator (porphyrin backbone) was metalated with Sn(IV) behaving as the hinge and allowing the introduction of the handle.[35] The metalation of **30** followed by in situ hydrolysis of the complex **30**-$SnCl_2$ was performed as previously described by Arnold et al.[42] Compound **30** reacted with an excess of hydrated tin(II) chloride in refluxing pyridine. The hydrolysis of the dichloro complex **30**-$SnCl_2$ leading to the dihydroxy complex **32** (Scheme 5) was achieved in 50% yield by addition of ammonia in the reaction medium followed by chromatography on alumina.

The dihydroxy tin complex **33** was synthesized following a similar procedure. However, since the use of chromatography to hydrolyze **31**-$SnCl_2$ was found to be inefficient, its formation required two steps. Following reported procedures[43] the reaction of **31** with an excess of $SnCl_2 \cdot 2H_2O$ afforded the dichloro complex **34** in 81% yield. The hydrolysis of the latter was performed in 81% yield using K_2CO_3 in a H_2O/THF mixture.

Synthesis of Model Porphyrins Bearing 3-Methoxyphenol as Axial Ligands. To study both the reactivity and the structural features of tin porphyrins bearing two resorcinol groups in apical positions, 3-methoxyphenol was used as a model axial ligand (Scheme 6). The substitution of the hydroxo ligands by 3-methoxyphenol in both compounds **32** and **33** was achieved following the reported procedures

(39) Nakamura, Y.; Takeuchi, S.; Ohgo, Y.; Yamaoka, M.; Yoshida, A.; Mikami, K. *Tetrahedron* **1999**, *55*, 4595–4620.
(40) Adler, A. D.; Longo, F. R.; Finarelli, J. D.; Goldmacher, J.; Assour, J.; Korsakoff, L. *J. Org. Chem.* **1967**, *32*, 476–476.
(41) Meng, G. Z. G.; James, B. R.; Skov, K. A. *Can. J. Chem.* **1994**, *72*, 1894–1909.
(42) Arnold, D. P. *J. Chem. Educ.* **1988**, *65*, 1111–1112.
(43) (a) Jo, H. J.; Jung, S. H.; Kim, H.-J. *Bull. Korean Chem. Soc.* **2004**, *25*, 1869–1873. (b) Crossley, M. J.; Thordarson, P.; Wu, R. A. S. *J. Chem. Soc., Perkin Trans. 1* **2001**, *18*, 2294–2302.

Table 1. Selected ^{1}H-NMR (300 MHz, $CDCl_3$) Chemical Shifts (δ, ppm) for 3-Methoxyphenol, **35**, and **36**

	H_α	H_β	H_γ	H_δ
3-methoxyphenol	6.44	6.44	7.14	6.51
35	1.43	1.50	5.53	5.37
36	1.41	1.48	5.53	5.38

by Langford et al.[44,45] Upon refluxing compounds **32** or **33** with an excess of 3-methoxyphenol in $CHCl_3$, complexes **35** and **36** were obtained after recrystallization in 85% and 78% yield, respectively.

The structural features of both **35** and **36** were studied in solution by ^{1}H NMR and in the solid state by X-ray diffraction on single crystals.

In solution, as expected,[35,46] owing to the magnetic anisotropy of the porphyrin, the ^{1}H NMR spectra of both compounds exhibit significant upfield shifts of the proton signals belonging to the mono protected resorcinol moiety. In particular, protons α and β (Scheme 6) display a chemical shift difference of about 5 ppm (Table 1). Furthermore, as expected, couplings between the two ^{117}Sn and ^{119}Sn isotopes and the β-pyrrolic protons, enabling the assignment of the signals, were also observed.

The solid-state structures of both complexes **35** and **36** were determined by single-crystal X-ray diffraction. Compounds **35** and **36** are *iso*structural (monoclinic system, $P2/c$ space group). Selected bond lengths and angles of **35** and **36** are given in Table 2. In both cases, the crystal contains only the complex, and no solvent molecules are present (Figure 3). The porphyrin core is almost perfectly planar, and the Sn atom is located almost at the center of the four pyrrolic units (Sn−N ca. 2.09 Å; NSnN ca. 89.9° to 90.1° (*cis*), 179.9° (*trans*)). The Sn(IV) cation is six-coordinated by four N atoms of the porphyrin and two O atoms of the two resorcinol groups (Sn−O ca. 2.05 Å). The coordination geometry is essentially octahedral with an OSnO angle of 179.9° and OSnN angles in the range 88.0 to 92.0°. The two axial ligands adopt a *trans* configuration to the tin atom and an *anti* arrangement of the two phenol groups. The four aromatic *meso* substituents are tilted with respect to the porphyrin plane (C−C−C−C dihedral angles +72.8°, +67.6°, −63.3°, and −68.1°). The mean plane of the phenol groups shows an angle of about 36° with respect to the porphyrin plane. The parameters observed in the solid-state structures of **35** and **36** are similar to those already reported for other tin porphyrin complexes.[45−48]

Synthesis of Compound 1. The synthesis of the molecular gate **1** was achieved by reaction of **33** with a small excess of **9** in $CHCl_3$ at RT. The evolution of the reaction was monitored by ^{1}H NMR. The pure compound **1** was obtained in 97% yield after 18 days. As previously reported by us in a communication,[33] the latter was fully characterized both in solution by NMR spectroscopy and in the solid state by X-ray diffraction on single crystals.

Synthesis of Compound 2. Compound **2** was synthesized by reaction of **33** with a small excess of **8** in dichloromethane at RT. Completion of the reaction was monitored by ^{1}H NMR. Indeed, the chemical shifts of the protons located on the phenoxo units (H_a, H_b, H_c, H_d, Scheme 1) and on the pyridine moiety (H_g, H_h, H_f) belonging to the handle are affected by the magnetic anisotropy of the porphyrin ring. As expected, whereas protons located on the resorcinol moieties are considerably upfield shifted, those corresponding to the pyridyl unit are only slightly affected by the presence of the porphyrin core (Table 3). After 6 days, compound **2** was obtained by recrystallization from a mixture of toluene and *n*-hexane in 75% yield.

Synthesis and Solid-State Structural Characterization of Compounds 3 and 4. The synthesis of both complexes was achieved at RT in 96% and 92% yield, respectively, by reaction of **32** with **8** or **9** in chloroform. Again, the completion of the reaction was monitored by ^{1}H NMR considering the chemical shifts of the protons located on the phenoxo and on the pyridine units (Table 3). Interestingly, for both **3** and **4**, the rotation of the handle around the hinge is not hindered as the signal corresponding to the β-pyrrolic protons, easily assigned because of the Sn−H coupling, appeared as a singlet.

In the crystalline phase, both compounds **3** (Figure 4a) and **4** (Figure 4b) were characterized by X-ray diffraction on single crystals. The latter were obtained by vapor diffusion of *n*-hexane into a toluene solution containing the complex.

Whereas, compounds **1** and **3** are *iso*structural, compounds **3** and **4** are not *iso*structural. Indeed, whereas for **3**, crystals (triclinic, $P\bar{1}$) only contain the molecular unit, **4** crystallizes in the orthorhombic system (space group $P2$) as a hexane solvate. However, the geometric parameters of the porphyrin core for both compounds are only slightly different (see Table 2). The structural features are similar to those observed for **1**. The Sn atom is located almost at the center of the porphyrin ring and adopts an almost octahedral geometry. No distortion of the planarity of the porphyrin is observed. The four phenyl groups are tilted with respect to the porphyrin plane (C−C−C−C dihedral angles +55.3°, −63.3°, −65.1°, and −72.0° for **3** and +70.1°, +61.0°, −69.3°, and −71.0° for **4**). For both structures, a fragment of the polyethyleneglycol chain is disordered.

The two solid-state structures show that both spacers connecting the two resorcinol moieties to the pyridine unit are long enough to allow free rotation of the handle around the hinge as indeed observed in solution (see above). However, inspection of CPK models as well X-ray structures clearly shows that, in the case of **4**, for the inline disposition of the N atom of the pyridine moiety of the handle and the C atom of one of the phenyl groups of the porphyrin, the distance is too short to permit the binding of a metal cation such as silver adopting the linear coordination geometry, whereas for **3**, the distance seems to be perfectly adapted for such a process. For that reason, the gate **1** bearing the same handle as **3** was prepared.[33] Furthermore, compound **2** was synthesized to confirm the hypothesis made above on the length of the handle.

(44) Fallon, G. D.; Langford, S. J.; Lee, M. A. P.; Lygris, E. *Inorg. Chem. Commun.* **2002**, *5*, 715–718.
(45) Fallon, G. D.; Lee, M. A. P.; Langford, S. J.; Nichols, P. J. *Org. Lett.* **2002**, *4*, 1895–1898.
(46) Langford, S. J.; Lee, M. A. P.; Macfarlane, K. J.; Weigold, J. A. *J. Inclusion Phenom.* **2001**, *41*, 135–139.
(47) Fallon, G. D.; Lee, M. A. P.; Langford, S. J. *Acta Crystallogr., Sect. E* **2001**, *57*, m564–m565.
(48) Nimri, S.; Keinan, E. *J. Am. Chem. Soc.* **1999**, *121*, 8978–8982.

Table 2. Selected Bond Distances and Angles for Compounds **1**, **3**, **4**, **6**, **35**, and **36**

	d_{Sn-O} (Å)	d_{Sn-N} (Å)	Φ_{OSnO} (deg)	Φ_{NSnO} (deg)	$\Phi_{NSnN\ trans}$ (deg)	$\Phi_{NSnN\ cis}$ (deg)
1[a]	2.052(4), 2.058(4)	2.096(5), 2.104(5), 2.106(5), 2.107(5)	176.9	87.2−92.1	179.0−179.7	89.6−90.6
3	2.050(10), 2.051(11)	2.089(12), 2.090(10), 2.104(12), 2.105(11)	175.7	86.6−92.5	178.4	89.3−91.2
4	2.040(4), 2.062(4)	2.086(4), 2.089(4), 2.095(4), 2.097(4)	179.0	88.0−92.6	179.2−179.3	89.5−90.5
6	2.071(3), 2.078(3)	2.104(3), 2.112(3), 2.112(3), 2.123(3)	178.3	88.4−92.9	178.6−179.3	89.8−90.4
35	2.049(3),	2.090(3), 2.094(3)	180.0	88.0−91.9	180.0	89.8−90.1
36	2.064(5)	2.105(5), 2.110(5)	180.0	88.1−91.9	180.0	89.6−90.4

[a] Previously reported, see ref 33.

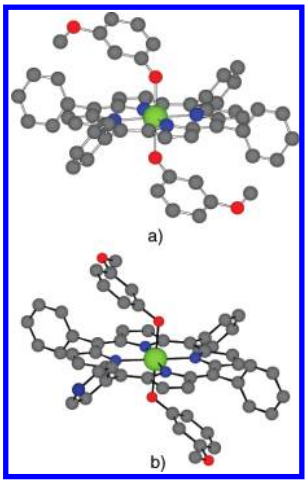

Figure 3. Crystal structures of **35** (a) and **36** (b). For the latter, the pyridine unit is disordered over 4 positions. H atoms are omitted for the sake of clarity. For bond distances and angles, see text and Table 2.

Table 3. Selected ^{1}H-NMR (300 MHz, $CDCl_3$) Chemical Shifts (δ, ppm) for **3**−**6** and **7**−**9**

	H_a	H_b	H_c	H_d	H_f	H_g	H_h
3	1.38	1.53	5.53	5.38	4.74	7.34	7.42
4	1.33	1.55	5.51	5.35	4.76	7.45	7.70
5	1.30	1.51	5.55	5.38			
6	1.35	1.59	5.53	5.39			
7	6.49	6.42[a]	7.06	6.42[a]			
8	6.42[a]	6.42[a]	7.04	6.42[a]	4.67	7.35	7.65
9	6.43[a]	6.43[a]	7.07	6.43[a]	4.67	7.37	7.67

[a] Multiplet.

Synthesis of Compound 5. Compound **5** was synthesized by reaction of **7** with compound **33** in dichloromethane at RT for 4 days and was obtained in 78% yield. As for the previous cases mentioned above, the completion of the reaction was monitored by ^{1}H NMR. Coordination of the handle to the tin atom causes substantial upfield shifts of the proton signals belonging to the phenoxo units (H_a, H_b, H_c, H_d, Table 3). The β-pyrrolic protons, easily assigned because of the Sn−H coupling, are not differentiated upon coordination of the handle to the tin atom indicating a free rotation of the handle around the hinge.

Synthesis and Solid-State Structural Characterization of Compound 6. The synthesis of **6** was achieved following a similar procedure as the one described above. In chloroform, the condensation of **7** with compound **32** at RT afforded the compound **6** in 85% yield. Compound **6** exhibits the similar spectral characteristics as compound **5** (see Table 3).

The solid-state structure of **6** was investigated by X-ray diffraction on single crystals, the latter being obtained by vapor diffusion of *n*-hexane into a toluene solution of **6**. The compound **6** crystallizes (triclinic, $P\bar{1}$) as a toluene hemisolvate with two porphyrin units and one toluene molecule in the unit cell (Figure 5). The geometric parameters of the porphyrin moiety are similar to those observed for the compounds described above (see Table 2). The porphyrin core is almost planar. The Sn atom, located in the center of the porphyrin ring, is hexacoordinated and surrounded by 4 N atoms (d_{Sn-N}

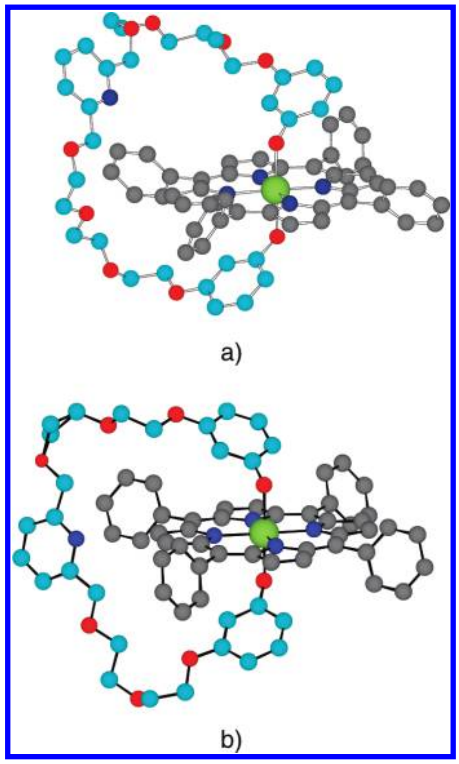

Figure 4. Solid-state structures of **3** (a) and **4** (b). In both structures, a fragment of the polyethyleneglycol units was found to be disordered. H atoms and solvent molecules are omitted for the sake of clarity. For bond distances and angles, see Table 2.

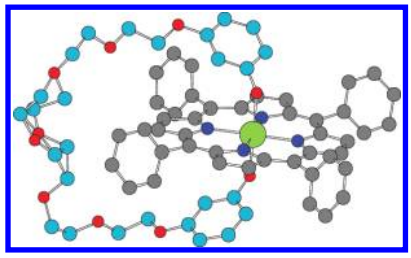

Figure 5. Solid-state structure of **6**. A fragment of the hexaethyleneglycol unit was found to be disordered. Solvent molecules and H atoms are omitted for the sake of clarity. For bond distances and angles, see Table 2.

in the range of 2.104 to 2.123 Å) and two O atoms (d_{Sn-O} of 2.071 and 2.078 Å).

Stability of the Sn−O bond in the Presence of Acids. The compound **1** was designed as a molecular gate based on the simultaneous binding of silver cation by both pyridine units located on the stator and on the handle. Interestingly, by considering the two pyridines as basic sites, another alternative consisting in closing the gate by a proton may also be envisaged. In that case, the locking of the handle to the stator would take place by H-bonding through the formation of a pyridinium-pyridine complex. Although the stability of Sn porphyrin complexes in acidic media was established, that is, the demetalation occurs only under harsh conditions,[35] to the best of our knowledge, in the presence of competitive ligands, no systematic study in solution dealing with the stability of the axial Sn−O bond within phenate complexes has been reported. To test our idea, we had first to study the stability of the axial Sn−O bonds in the presence of different acids. It should be noted that for such investigation, one needs to consider both the strength of the acid and the propensity of its conjugated base (anion) to bind to the Sn atom complexed by the porphyrin core. Indeed, one could expect a proton-catalyzed substitution of the axial ligand (phenoxide type) by the anion of the acid. Most of the studies reported so far deal essentially with the stability of aryloxo complexes under hydrolytic conditions.[35] Nimri et al. reported that a tin porphyrin complex bearing one α-naphthoxy and one chloride anion as axial ligands was satisfactorily stable during 48 h under physiological conditions (50 mM phosphate buffer, pH 7.4, $[Cl^-]$ = 0.1 M, 37 °C).[48] However, the solution was nevertheless composed of a mixture of mono- and dichloro complexes.

Complex **35** was used as a model. The reaction in the presence of variable amounts of different acids in CD_3CN or $CDCl_3$ at 25 °C, was monitored by ^1H NMR by observing the shifts associated with signals related to the protons of resorcinol groups (γ, δ, and ε) and to the β-pyrrolic protons (Scheme 6). Both HBF_4 and trifluoroacetic acid (TFA) were used. They both induced the decoordination of the monoprotected resorcinol moiety and its substitution by fluoro or trifluoroacetate anions respectively. For the addition of 1 or 2 equiv of HBF_4 or TFA, the ^1H NMR study revealed the disappearance of the complex **35** and the concomitant generation of the 3-methoxyphenol as well as complexes **37** (signal at 9.43 ppm[49])and **38** (signals at 9.33 ppm) (Scheme 7). For a detailed description of ^1H NMR spectra see Figures S1 (HBF_4) and S2 (TFA) in the Supporting Information.

Furthermore, the solid state structures of both species were determined by X-ray diffraction on single crystals (see the X-ray section in the Supporting Information) formed in the NMR tube upon slow evaporation (Figures 6 and 7). For the description of both structures see the Supporting Information. The presence of F^- anion results from the dissociation of BF_4^-anion into BF_3 and F^-. The solid-state structure of **37** consists of the difluorocomplex **37** and four CH_3CN solvent molecules. The structure obtained here is similar in terms

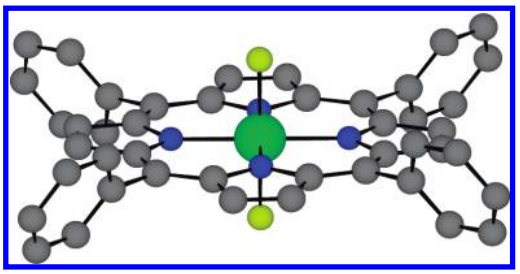

Figure 6. Crystal structure of **37**. Solvent molecules and H atoms are omitted for the sake of clarity. For bond distances and angles see text.

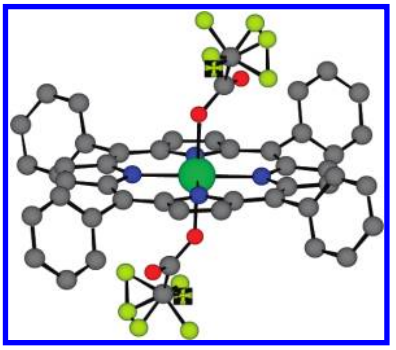

Figure 7. Crystal structure of **38**. The CF_3 groups are disordered over two positions. Solvent molecules and H atoms are omitted for the sake of clarity. For bond distances and angles see text.

Scheme 7. Structures of Compounds **37** and **38**

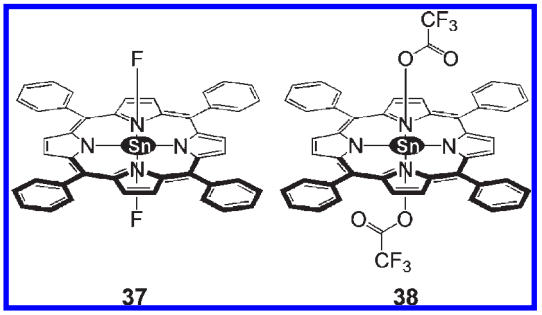

of geometric parameters to the one already reported for the same complex.[50] However, the two structures differ by the presence of CH_3CN solvent molecule in the present case which leads to another crystal system, as well as another space group. For the compound **38**, no solvent molecules were found to be included in the crystal (triclinic, $P\bar{1}$).

To study the role played by the binding ability of the anion, weakly coordinating sufonate derivatives were considered. Indeed, such anions have been described previously as weak ligands for tin porphyrins.[35] Thus, trifluoromethanesulfonic acid (TfOH) and methanesulfonic acid (MsOH) were tested. In the case of **35**, the addition of TfOH leads to a rapid equilibrium between different porphyrins (presence of five singlets exhibiting Sn−H coupling, Figure 8). The singlet corresponding to the β-pyrrolic protons of the starting material (δ = 9.09 ppm) completely disappeared after addition of 3 equiv of TfOH. In the meantime, a singlet corresponding to the triflate complex (**30**-Sn$(TfO)_2$) appeared

(49) Arnold, D. P.; Morrison, E. A.; Hanna, J. V. *Polyhedron* **1990**, *9*, 1331–1336.

(50) Arnold, D. P.; Tiekink, E. R. T. *Polyhedron* **1995**, *14*, 1785–1789.

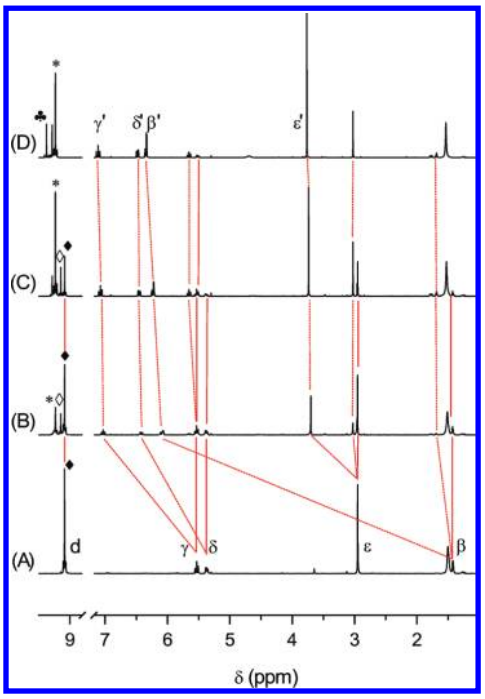

Figure 8. Portions of the ^{1}H NMR spectra (300 MHz, $CDCl_3$, 25 °C) and assignment of signals between 1.1−7.2 ppm and 8.8−9.5 ppm for the complex **35** in the presence of 0 (A), 1 (B), 2 (C), and 3 (D) equiv of triflic acid. For assignment of H-atoms see Scheme 6. ♦ refers to the starting porphyrin **35**, ◊ and * refer to two new porphyrin derivatives, and the black clover leaf refers to **30**-Sn(TfO)$_2$.

at 9.37 ppm.[51] Upon addition of 1 or 2 equiv of TfOH, 3 singlets are observed for the methoxy protons (ε, Scheme 6) of resorcinol moieties indicating the presence of 3 different species. Two out of the three signals correspond to the free 3-methoxyphenol (δ = 3.77 ppm) and the initial complex **35** (δ = 2.95 ppm) respectively. The third one corresponds to a mixed complex bearing one methoxyphenol and another axial ligand (TfO^- or OH^-). When 3 equiv of TfOH are added, the signal at 2.95 ppm corresponding to **35** disappeared implying the substitution of both monoprotected resorcinol ligands by TfO^- or OH^- groups. In solution, the relative concentration of these three different species may be quantified by considering the integrations of the signals corresponding to protons ε in **35** (δ = 2.95 ppm), the mixed complex (δ = 3.04 ppm) and the free (δ = 3.77 ppm) species (Table S3, see Supporting Information).

Since the complex **36** bears a pyridine group attached to the porphyrin moiety, the effect of the addition of TfOH was also studied on this compound. The same type of behavior was again observed (Figure S3, see Supporting Information). Indeed, upon addition of TfOH to **36**, the decoordination of both methoxyphenolate type ligands and their replacement by TfO^- or OH^- anions take place (Table 4).

The behavior of complex **36** in the presence of different equivalents of MsOH, a weaker acid than TfOH, was also studied under the same conditions (Figure S4, see Supporting Information). Unfortunately, again, the intensity of the signals related to the free 3-methoxyphenol is enhanced upon increasing the number of equivalents of

(51) Smith, G.; Arnold, D. P.; Kennard, C. H. L.; Mak, T. C. W. *Polyhedron* **1991**, *10*, 509–516.

Table 4. Effect of the Addition of Triflic Acid to a $CDCl_3$ Solution of **36** on the Relative Percentage (%) of the Three Different Species Bearing 3-Methoxyphenol Unit

	36	mixed complex	free 3-methoxyphenol
1 equiv	46%	13%	41%
2 equiv	5%	28%	67%
3 equiv	0%	27%	73%

Table 5. Effect of the Addition of Methanesulfonic Acid to a $CDCl_3$ Solution of **36** on the Relative Percentage (%) of the Three Different Species Bearing 3-Methoxyphenol Unit

	36	mixed complex	free 3-methoxyphenol
1 eq	47%	11%	42%
2 eq	18.5%	18.5%	63%
3 eq	3%	18%	79%

acid added. Furthermore, three signals at −0.41 ppm, −0.59 ppm, and −0.63 ppm are observed. These correspond to methyl protons of the methanesulfonate anion indicating the substitution of the methoxyphenol ligands by sulfonate anions. Again, it is possible to determine the relative amounts of each species in solution (Table 5).

Surprisingly, independent of the nature of the acid added (MsOH or TfOH), the percentages of the three species present in solution are roughly the same for all three numbers of equivalents added. This indicates that the amount of the different complexes in solution is not only related to the pK_a values of the acids added (p$K_{aMsOH} \approx -2$, p$K_{aTfOH} \approx -13$) but also depends on the binding propensity of the conjugated base. This observation is in agreement with Langford's statement.[46] However, it is the opposite of what was reported by Sanders et al. who observed a linear pK_a dependence for carboxylate anions.[52] Thus, HBF_4, TFA, TfOH, and MsOH acids are not suitable as proton sources since all four, although with not the same efficiency, lead to the substitution of phenoxy type ligands by their counterions.

Binding of Ag^+ Cation to Compounds 1−6. As demonstrated above, the use of acids as external stimulus to lock the gate by H-bonding is not feasible. However, as reported earlier in a communication,[33] the locking process may be achieved by silver cation in the case of **1**. The role of Ag^+ cation as an external stimulus was investigated by ^{1}H NMR for compound **2** possessing a shorter handle when compared to compound **1** as well as for prototypes **3**−**6**. The choice of silver cation as external stimulus was based on the following rationale. Owing to its d^{10} electronic configuration, silver cation exhibits a rather loose geometric demand and, as often observed (see for example refs 53−58), in the presence of two pyridine moieties, it adopts a linear coordination geometry

(52) Hawley, J. C.; Bampos, N.; Sanders, J. K. M.; Abraham, R. J. *Chem. Commun.* **1998**, 661–662.
(53) Kondo, M.; Kimura, Y.; Wada, K.; Mizutani, T.; Ito, Y.; Kitagawa, S. *Chem. Lett.* **2000**, 818–819.
(54) Carlucci, L.; Ciani, G.; Proserpio, D. M.; Porta, F. *Angew. Chem., Int. Ed.* **2003**, *42*, 317–322.
(55) Bosch, E.; Barnes, C. L. *Inorg. Chem.* **2001**, *40*, 3234–3236.
(56) Bowmaker, G. A.; Effendy; Lim, K. C.; Skelton, B. W.; Sukarianingsih, D.; White, A. H. *Inorg. Chim. Acta* **2005**, *358*, 4342–4370.
(57) Greco, N. J.; Hysell, M.; Goldenberg, J. R.; Rheingold, A. L.; Tor, Y. *Dalton Trans.* **2006**, 2288–2290.
(58) Engelhardt, L. M.; Pakawatchai, C.; White, A. H. *J. Chem. Soc., Dalton Trans.* **1985**, 117–123.

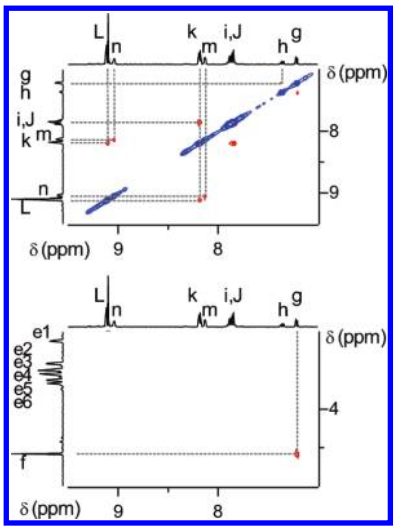

Figure 9. Portions of the 2D Roesy correlation (^{1}H−^{1}H NMR, CD_3CN, 500 MHz, 25 °C) of **1** in the absence of any metal cation.

perfectly suited for the present design principle. Moreover, the binding affinity of pyridine for silver is high enough to afford a stable complex. The latter is labile allowing thus reversible coordination/decoordination processes leading to closing and opening of the gate. Finally, Ag(I) is diamagnetic and enables ^{1}H NMR studies of such dynamic systems.[59,60] As reported earlier,[33] in the case of the molecular gate **1**, free rotation of the handle around the stator takes place in the absence of any stimulus. Indeed, the only correlation peaks observed on the Roesy spectrum of **1** correspond to chemically linked protons (H_m and H_n, H_h and H_g, H_f and H_g, Figure 9, Scheme 1). This was explained by fast rotation of the handle around the Sn−O bond. The same behavior is also observed for the prototype **2**.

For the gate **1**, in the presence of 1 or 2 equiv of AgOTf, the closing of the gate results in the appearance of new correlation peaks owing to spatial proximity of the two pyridine units (correlation peaks between proton H_n of the stator and protons H_{e4}, H_{e5}, H_{e6}, and H_f of the handle, see Figure S6 in Supporting Information). Compound **2** was also studied in the presence of Ag^+ to establish the role played by the length of the handle on the simultaneous binding of the cation by both pyridine units. The titration of **2** with different equivalents of Ag^+ was investigated by ^{1}H NMR in CD_3CN. The same procedure as for **1** was used.[33] Binding of Ag^+ by **2** induces small downfield shifts of the signal of H_f protons (Scheme 1, Figure 10) as well as proton signals belonging to both pyridine moieties (H_g, H_h, H_m, and H_n, Scheme 1, Figure 11). The signals assigned to the β-pyrrolic protons are also affected by the binding process. It is worth noting that in the case of **2**, the difference in the chemical shift observed in the presence of up to 2 equiv of silver cation is much less pronounced for all protons than in the case of **1** (Table 6). Moreover, ROESY experiments (Figure S7, see Supporting Information) performed when 1 equiv of Ag^+ was added

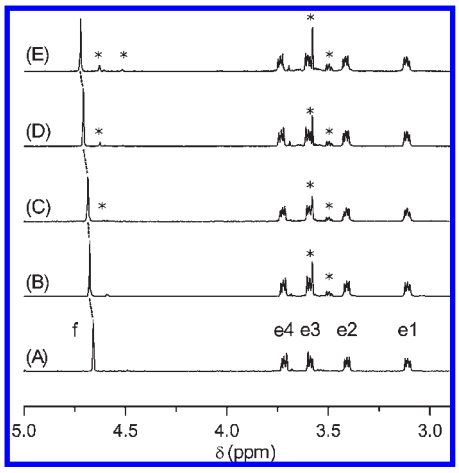

Figure 10. Portions of the ^{1}H NMR spectra (CD_3CN, 400 MHz, 25 °C) of **2** in the presence of 0 (A), 0.5 (B), 1 (C), 2 (D), and 3 (E) equiv of AgOTf and assignments of signals (see Scheme 1) between 3 and 5 ppm. * refers to new species formed.

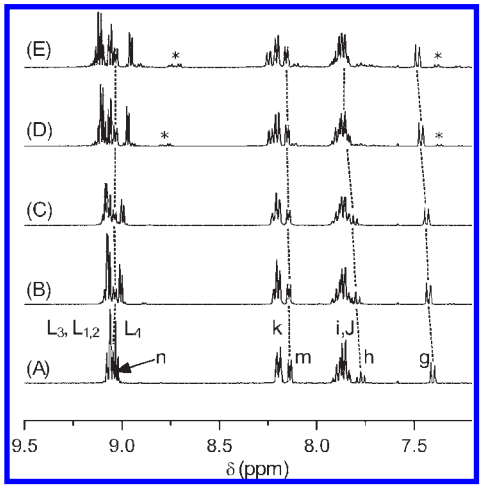

Figure 11. Portions of the ^{1}H NMR spectra (CD_3CN, 400 MHz, 25 °C) of **2** in the presence of 0 (A), 0.5 (B), 1 (C), 2 (D), and 3 (E) equiv of AgOTf and assignments of signals (see Scheme 1) between 7 and 9.5 ppm. * refers to new species formed.

Table 6. Selected ^{1}H-NMR Chemical Shifts Difference (in Hz) of Protons Located on the Pyridine Moieties for **1**−**5** in the Presence of 0 and 2 equiv of AgOTf

	H_g	H_h	H_m	H_n
1[a]	155	> 255*	> 60*	70
2[a]	25	> 24*	5	3
3[b]	12	24		
4[b]	> 6*	6		
5[c]			6	12

[a] CD_3CN, [b] CD_3CN/CD_2Cl_2 8/2, [c] CD_3CN/CD_2Cl_2 6/4, * Signals hidden under other peaks.

showed no correlation peak between protons H_n and H_f indicating the absence of spatial proximity of the two pyridines. This may be due to the absence of the simultaneous binding of the cation by both pyridines. This observation correlates also with the small shifts observed upon addition of the cation to the prototype **2**.

It is worth noting that whereas for **1**, the addition of increasing amounts of Ag^+ cation leads to a single species, that is, observation of a single set of signals, in the case of

(59) Bogdan, N.; Grosu, I.; Benoît, G.; Toupet, L.; Ramondenc, Y.; Condamine, E.; Silaghi-Dumitrescu, I.; Plé, G. *Org. Lett.* **2006**, *8*, 2619–2622.
(60) Chou, T.-C.; Hwa, C.-L.; Lin, J.-J.; Liao, K.-C.; Tseng, J.-C. *J. Org. Chem.* **2005**, *70*, 9717–9726.

2, the addition of the cation generates new species which may correspond to polynuclear species and complexes bearing CH_3CN as secondary ligand (Figures 10 and 11). The formation of these entities probably originates from the shortening of the handle and consequently the distance between the two pyridine units located respectively on the stator and the handle preventing thus the formation of the desired complex. This is in agreement with the ROESY experiment described above.

The effect of binding of silver cation by the other four prototypes **3**−**6** was also studied. For compounds **3**−**5** bearing a pyridine unit on the handle (for **3** see Figure S8 and Table S6 and for **4** see Figure S9 and Table S7 in the Supporting Information) or on the stator (**5**, Figure S10 and Table S8 in the Supporting Information), in the presence of Ag^+ cation, slight differences in the chemical shifts were observed indicating some interactions between the cation and the pyridine unit (Table 6). In the case of the prototype **6**, bearing no coordination site, as expected, no change in the ^1H NMR signals was observed (Figure S11 and Table S9 in the Supporting Information).

Conclusions

The design of molecular gates is presented based on porphyrin cores bearing at the *meso* positions either phenyl or pyridyl groups acting as a stator, octahedral Sn(IV) cation located at the center of the porphyrin behaving as a hinge, and different resorcinol based handles connected to the porphyrin through Sn−O axial bonds. All parts of the molecular system have been finely tuned. For their preparation, a rather long stepwise synthetic strategy was developed. In addition to classical characterization techniques, 7 of the newly reported derivatives have been structurally studied in the crystalline phase by X-ray diffraction methods on single crystals. The stability of two model Sn-porphyrin complexes bearing two monoprotected resorcinol moieties in the presence of different acids was studied in solution by ^1H NMR. Both the strength of the acid and the coordination propensity of the anion were found to be important. Indeed, upon addition of different acids (HBF_4, TFA, MsOH, TfOH), the substitution of the axial resorcinol group by the anion was observed. This indicated that a proton can not be used as an external stimulus. The gate was designed to function with silver cation as effector. The systematic study carried out on the gate **1** and its analogues **2**−**6** (prototypes) clearly demonstrated the need for the simultaneous presence of the two coordinating sites on the stator and on the handle. Furthermore, it allowed to determine the optimum distance between the two parts, that is, the length of the handle, for the binding of the cation by both sites.

The design of other analogue systems based on porphyrin units bearing at the *meso* positions different coordination sites is currently under investigation. Modification of the handle by increasing the denticity of its coordinating site for example should allow the use of transition metal cations to control the locking/unlocking of the gate. Work along these lines is currently ongoing.

Experimental Section

General Procedures. Solvents were dried using standard techniques: THF and CH_2Cl_2 were distilled over Na and CaH_2, respectively. Pyridine and Et_3N were dried over KOH. Ethyl acetate, CH_3CN, and $CHCl_3$ were dried over molecular sieves. All air and water sensitive experiments were carried out under argon atmosphere using standard vacuum line techniques. All chemicals were obtained commercially and used without further purification, except pyrrole which was purified over an alumina column before use.

^1H-and ^{13}C NMR spectra were acquired on either a Bruker AV 300 (300 MHz), a Bruker AV400 (400 MHz), or a Bruker AV 500 (500 MHz) spectrometer, with the deuterated solvent as the lock and residual solvent as the internal reference. Absorption spectra were recorded using an Uvikon XL spectrophotometer. Elemental analyses were performed by the Service de Microanalyses, ULP, Strasbourg. Matrix assisted laser desorption ionization time-of-flight (MALDI-TOF) spectra were taken on a Bruker autoflex II TOF TOF (equipped with a nitrogen laser and used in reflectron mode) with dithranol (1,8,9-trihydroxyanthracene) as matrix. A microTOF LC (Bruker Daltonics, Bremen) spectrometer equipped with an electrospray source was used for the electrospray mass spectrometry measurements (ES-MS).

Synthesis. Here, only the synthetic procedures for the preparation of the final compounds **1**−**6** are given. The detailed syntheses of all the other 27 intermediates (**7**-**34**) as well as complexes **35** and **36** are described in the Supporting Information.

Compound 1. To a solution of **33** (25.6 mg, 0.033 mmol, 1 equiv) in dry $CHCl_3$ (25 mL) was added dropwise a solution of **9** (21.6 mg, 0.037 mmol, 1.1 equiv) in dry $CHCl_3$ (25 mL) at RT. The mixture was stirred at RT for 18 days. The evolution of the reaction was monitored by ^1H NMR. The solvent was then removed under vacuo. The crude product was recrystallized by slow diffusion of *n*-hexane (75 mL) into a toluene solution (17 mL) of the desired compound to afford purple crystals (42.2 mg, 97%). Single crystals suitable for X-ray diffraction were grown by vapor diffusion of *n*-hexane into a toluene solution containing the desired compound. ^1H NMR (CD_3CN, 500 MHz, 25 °C): δ (assignments according to COSY and ROESY 2D $^1H-^1H$ NMR experiments) 1.21 (t, $^4J = 2.3$ Hz, 2H, H_a,), 1.41 (ddd, $^3J = 8.0$ Hz, $^4J = 2.1$ Hz, $^4J = 0.8$ Hz, 2H, H_b), 3.12 (t, $^3J = 4.6$ Hz, 4H, H_{e1}), 3.41 (m, 4H, H_{e2}), 3.49 (m, 4H, H_{e3}), 3.55 (m, 4H, H_{e4}), 3.62 (m, 4H, H_{e5}), 3.67 (m, 4H, H_{e6}), 4.58 (s, 4H, H_f), 5.33 (ddd, $^3J = 8.2$ Hz, $^4J = 2.4$ Hz, $^4J = 0.8$ Hz, 2H, H_d), 5.50 (t, $^3J = 8.1$ Hz, 2H, H_c), 7.21 (d, $^3J = 7.8$ Hz, 2H, H_g,), 7.36 (t, $^3J = 7.8$ Hz, 1H, H_h), 7.83−7.90 (m, 9H, H_{i1}, H_{i2}, H_{J1}, H_{J2}), 8.13 (dd, $^3J = 4.1$ Hz, $^4J = 1.6$ Hz, 2H, H_m), 8.17−8.19 (m, 6H, H_{k1}, H_{k2}), 9.04 (dd, $^3J = 4.2$ Hz, $^4J = 1.5$ Hz, 2H, H_n), 9.09 (d, $^3J = 4.9$ Hz, 2H, H_{L4}), 9.10 (s, 4H, H_{L1}, H_{L2}), 9.12 (d, $^3J = 4.9$ Hz, 2H, H_{L3}). ^{13}C NMR (CD_3CN, 125 MHz): δ (assignments according to HSQC and HMBC 2D $^1H-^{13}C$ NMR experiments) 67.0 (C_{e1}), 69.9 (C_{e2}), 70.92 (C_{e6}), 70.9 (C_{e5}), 71.0 (C_{e3}), 71.1 (C_{e4}), 74.6 (C_f), 103.7 (C_a), 104.4 (C_d), 110.5 (C_b), 119.7 (C_p), 120.7 (C_g), 123.5 (C_s, C_w), 127.6 (C_c), 128.0 (C_{J1}, C_{J2}), 129.6 (C_{i1}, C_{i2}), 130.3 (C_m), 133.0 (C_{L4}), 133.9 (C_{L1}, C_{L2}), 134.1 (C_{L3}), 135.7 (C_{k1}, C_{k2}), 138.2 (C_h), 141.5 (C_t, C_x), 147.1 (C_u, C_v, C_r), 148.4 (C_q), 149.3 (C_n), 149.7 (C_o), 157.0 (C_{a2}), 158.9 (C_{a1}), 159.3 (C_{f1}). Labeling of the hydrogen and carbon atoms is given in the Supporting Information. UV−vis (CH_2Cl_2) λ max (nm) (ε, mol^{-1} L cm^{-1}) 425 (3.2×10^5), 560 (2.1×10^4), 600 (1.0×10^4). MALDI-TOF MS: *m*/*z* obsd 1319.43, calcd 1319.39 [$(M + H)^+$; $M = C_{74}H_{66}N_6O_{10}Sn$].

Compound 2. To a solution of **33** (30.3 mg, 0.040 mmol, 1 equiv) in dichloromethane (60 mL) was added a solution of **8** (20.9 mg, 0.042 mmol, 1.05 equiv) in dichloromethane (20 mL). The resulting solution was stirred at RT during 6 days. After removal of the solvent, the dark red residue was recrystallized by slow diffusion of *n*-hexane into a toluene solution containing the desired compound (37 mg, 75%). ^1H NMR (CD_3CN/CD_2Cl_2 8/2, 500 MHz): δ (assignments according to COSY and ROESY 2D $^1H-^1H$ NMR experiments) 1.18 (t, $^4J = 2.3$ Hz, 2H, H_a), 1.40 (ddd, $^3J = 8.0$ Hz, $^4J = 2.1$ Hz, $^4J = 0.9$ Hz, 2H, H_b), 3.09−3.14

(m, 4H, H_{e1}), 3.39−3.44 (m, 4H, H_{e2}), 3.58−3.62 (m, 4H, H_{e3}), 3.70−3.74 (m, 4H, H_{e4}), 4.66 (s, 4H, H_f), 5.31 (dd, ^3J = 7.2 Hz, ^4J = 2.5 Hz, 2H, H_d), 5.49 (t, ^3J = 8.0 Hz, 2H, H_c), 7.40 (d, ^3J = 7.8 Hz, 2H, H_g), 7.76 (t, ^3J = 7.8 Hz, 1H, H_h), 7.82−7.92 (m, 9H, $H_{i,J}$), 8.10−8.16 (m, 2H, H_m), 8.17 −8.22 (m, 6H, H_k), 9.02 (d, ^3J = 5 Hz, 2H, H_{L4}), 9.03 (m, 2H, H_n), 9.07 (s, 4H, $H_{L1,L2}$), 9.07 (d, ^3J = 6.5 Hz, 2H, H_{L3}). ^{13}C NMR (CD_3CN/CD_2Cl_2 8/2, 100 MHz): δ (assignments according to HSQC and HMBC 2D ^{1}H−^{13}C NMR experiments) 66.4 (C_{e1}), 69.0 (C_{e2}), 70.1 (C_{e4}), 70.8 (C_{e3}), 74.1 (C_f), 102.7 (C_a), 103.0 (C_d), 109.8 (C_b), 118.4 (Cp), 120.1 (Cg), 122.4 ($C_{s,w}$), 126.4 (C_c), 127.0 (C_k), 128.5 (C_J), 129.3 (C_m), 131.8 (C_{L4}), 132.8 ($C_{L1,L2}$), 133.0 (C_{L3}), 134.6 (C_i), 137.1 (C_h), 140.5 ($C_{t,x}$), 146.2 (C_q), 147.1 ($C_{r,u,v}$), 147.2 (C_o), 148.4 (C_n), 155.7 (C_{a1}), 157.4 (C_{a2}), 158.3 (C_{g1}). UV−vis (CH_2Cl_2) λ max (nm) (ε, mol^{-1} L cm^{-1}) 424 (2.2×10^5), 560 (1.5×10^4), 600 (0.8×10^4) MALDI-TOF MS: m/z obsd 1231.30, calcd 1231.34 [(M−H) $^+$; M = $C_{70}H_{58}N_6O_8Sn$].

Compound 3. To a solution of **32** (24.0 mg, 0.031 mmol, 1 equiv) in dry chloroform (10 mL) was added dropwise under argon a solution of **9** (20.0 mg, 0.034 mmol, 1.1 equiv) in dry chloroform (20 mL). The resulting mixture was stirred at RT during 6 days. The reaction was monitored by ^{1}H NMR. The solvent was removed in vacuo. The resulting powder was recrystallized by slow diffusion of *n*-hexane into a toluene solution of **3** to afford a crystalline violet powder (40.0 mg, 96%). Single crystals suitable for X-ray diffraction were grown by vapor diffusion of *n*-hexane into a toluene solution containing the desired compound. ^{1}H NMR ($CDCl_3$, 300 MHz): δ 1.38 (t, ^4J = 2.2 Hz, 2H, CH_{res}), 1.53 (dd, ^3J = 7.7 Hz, ^4J = 2.1 Hz, 2H, CH_{res}), 3.16 (t, ^3J = 5.0 Hz, 4H, CH_2O), 3.49 (t, ^3J = 5.0 Hz, 4H, CH_2O), 3.59 (m, 4H, CH_2O), 3.64 (m, 4H, CH_2O), 3.76 (m, 8H, CH_2O), 4.74 (s, 4H, $ArCH_2$), 5.38 (dd, ^3J = 8.1 Hz, ^4J = 2.2 Hz, 2H, CH_{res}), 5.53 (t, ^3J = 8.0 Hz, 2H, CH_{res}), 7.34 (d, ^3J = 7.5 Hz, 2H, CH_{Py}), 7.42 (t, ^3J = 7.7 Hz, 1H, CH_{Py}), 7.78 (m, 12H, $CH_{Ph\ meta/para}$), 8.19 (m, 8H, $CH_{Ph\ ortho}$), 9.07 (s, 8H, $CH_{\beta\text{-pyrrolic}}$, $^4J_{Sn-H}$ = 12.6 Hz). ^{13}C NMR ($CDCl_3$, 75 MHz): δ 66.2 (CH_2O), 69.6 (CH_2O), 70.5 (CH_2O), 70.7 (CH_2O), 70.8 (CH_2O), 70.9 (CH_2O), 74.2 (CH_2O), 103.2 (CH), 103.7 (CH), 110.4 (CH), 120.1 (CH), 121.8 (C_{quat}), 126.3 (CH), 126.9 (CH), 128.3 (CH), 132.5 (CH), 134.9 (CH), 137.2 (CH), 141.0 (C_{quat}), 147.2 (C_{quat}), 155.8 (C_{quat}), 157.0 (C_{quat}), 158.0 (C_{quat}). UV−vis (CH_2Cl_2) λ max (nm) (ε, mol^{-1} L cm^{-1}) 425 (3.2×10^5), 561 (2.0×10^4), 600 (1.3×10^4). Anal. Calcd. for $C_{75}H_{67}N_5O_{10}Sn$: C, 68.39; H, 5.13; N, 5.32. Found: C, 68.28; H, 5.11; N, 5.30. MALDI-TOF MS: m/z obsd 1318.36, calcd 1318.19 [(M+H)$^+$; M = $C_{75}H_{67}N_5O_{10}Sn$].

Compound 4. To a solution of **32** (42.1 mg, 0.055 mmol, 1 equiv) in dry chloroform (18 mL) was added dropwise under argon a solution of **8** (30.2 mg, 0.060 mmol, 1.1 equiv) in dry chloroform (34 mL). The resulting mixture was stirred at RT during 4 days. The reaction was monitored by ^{1}H NMR. After removal of the solvent, the resulting powder was recrystallized by slow diffusion of *n*-hexane into a toluene solution of **4** affording a crystalline dark red powder (62 mg, 92%). Single crystals suitable for X-ray diffraction were grown by vapor diffusion of *n*-hexane into a toluene solution containing the compound. ^{1}H NMR ($CDCl_3$, 300 MHz): δ 1.33 (t, ^4J = 2.3 Hz, 2H, CH_{res}), 1.55 (dd, ^3J = 7.9 Hz, ^4J = 1.8 Hz, 2H, CH_{res}), 3.15 (m, 4H, CH_2O), 3.48 (m, 4H, CH_2O), 3.65 (m, 4H, CH_2O), 3.75 (m, 4H, CH_2O), 4.76 (s, 4H, $ArCH_2$), 5.35 (ddd, ^3J = 8.0 Hz, ^4J = 2.4 Hz, ^4J = 0.9 Hz, 2H, CH_{res}), 5.51 (t, ^3J = 8.0 Hz, 2H, CH_{res}), 7.45 (d, ^3J = 7.6 Hz, 2H, CH_{Py}), 7.70 (t, ^3J = 7.6 Hz, 1H, CH_{Py}), 7.78 (m, 12H, $CH_{Ph\ meta/para}$), 8.20 (m, 8H, $CH_{Ph\ ortho}$), 9.03 (s, 8H, $CH_{\beta\text{-pyrrolic}}$, $^4J_{Sn-H}$ = 12.4 Hz). ^{13}C NMR ($CDCl_3$, 75 MHz): δ 66.4 (CH_2O), 69.4 (CH_2O), 70.2 (CH_2O), 71.0 (CH_2O), 74.4 (CH_2O), 103.3 (CH), 110.4 (CH), 120.4 (CH), 121.7 (C_{quat}), 126.2 (CH), 126.9 (CH),128.2 (CH), 129.0 (CH), 132.4 (CH), 134.9 (CH), 137.2 (CH), 141.0 (C_{quat}), 147.2 (C_{quat}), 155.8 (C_{quat}), 157.0 (C_{quat}), 158.1 (C_{quat}). UV−vis (CH_2Cl_2) λ max (nm) (ε, mol^{-1} L cm^{-1}) 425 (3.0×10^5), 561 (1.9×10^4), 601 (1.1×10^4). MALDI-TOF MS: m/z obsd 1230.31, calcd 1230.34 [(M+H)$^+$; M = $C_{71}H_{59}N_5O_8Sn$].

Compound 5. To a solution of **7** (6.1 mg, 0.013 mmol, 1 equiv) in dichloromethane (5 mL) was added **33** (10 mg, 0.013 mmol, 1 equiv). The resulting solution was stirred at RT for 4 days. After removal of the solvent, a violet powder was obtained which was recrystallized in a mixture of toluene/*n*-hexane (12.2 mg, 78%). ^{1}H NMR (CD_2Cl_2, 400 MHz): δ (assignments according to COSY and ROESY 2D ^{1}H−^{1}H NMR experiments) 1.28 (t, ^4J = 2.3 Hz, 2H, H_a), 1.53 (ddd, ^3J = 8.0 Hz, ^4J = 2.0 Hz, ^4J = 0.9 Hz, 2H, H_b), 3.14−3.16 (m, 4H, H_{e1}), 3.49−3.51 (m, 4H, H_{e2}), 3.60−3.63 (m, 4H, H_{e3}), 3.66−3.69 (m, 4H, H_{e4}), 3.71 (s, 8H, $H_{e5,e6}$), 5.38 (ddd, ^3J = 8.0 Hz, ^4J = 2.3 Hz, ^4J = 0.8 Hz, 2H, H_d), 5.55 (t, ^3J = 8.0 Hz, 2H), 7.86−7.93 (m, 9H, $H_{i,J}$), 8.19 (dd, ^3J = 4.2 Hz, ^4J = 1.5 Hz, 2H, H_m,), 8.27−8.29 (m, 3H, H_k), 9.11 (dd, ^3J = 3.6 Hz, ^4J = 1.2 Hz, 2H, H_n), 9.14 (d, ^3J = 4.8 Hz, 2H, H_{L3}), 9.21 (s, 4H, $H_{L1,L2}$), 9.23 (d, ^3J = 4.8 Hz, 2H, H_{L4}). ^{13}C NMR (CD_2Cl_2, 100 MHz): δ (assignments according to HSQC and HMBC 2D ^{1}H−^{13}C NMR experiments) 66.6 (C_{e1}), 69.5 (C_{e2}), 71.0 ($C_{e3,e4,e5,e6}$), 103.3 (C_a), 104.2 (C_d), 110.5 (C_b), 118.2 (C_p), 126.7 (C_c), 126.9 ($C_{s,w}$), 127.5 (C_i), 128.8 (C_J), 129.6 (C_m), 131.6 (C_q), 132.0 (C_{L3}), 132.6 ($C_{L1,L2}$), 132.8 (C_{L4}), 135.0 (C_k), 140.5 ($C_{t,x}$), 146.1 (C_r), 147.2 ($C_{u,v}$), 148.5 (C_o), 148.9 (C_n), 155.6 (C_{a2}), 157.1 (C_{a1}). UV−vis (CH_2Cl_2) λ max (nm) (ε, mol^{-1} L cm^{-1}) 425 (2.0×10^5), 560 (1.3×10^4), 600 (0.7×10^4). MALDI-TOF MS: m/z obsd 1198.17, calcd 1198.34 [(M+H$^+$); M = $C_{67}H_{59}N_5O_9Sn$].

Compound 6. To a solution of **32** (50.2 mg, 0.066 mmol, 1 equiv) in dry chloroform (20 mL) was added dropwise under argon a solution of **7** (33.8 mg, 0.073 mmol, 1.1 equiv) in dry chloroform (30 mL). The resulting mixture was stirred at RT during 5 days. The reaction was monitored by ^{1}H NMR. After removal of the solvent, the resulting powder was recrystallized by slow diffusion of *n*-hexane into a toluene solution of **6** affording a crystalline dark red powder (68.3 mg, 85%). Single crystals suitable for X-ray diffraction were grown by vapor diffusion of *n*-hexane into a toluene solution containing the compound. ^{1}H NMR ($CDCl_3$, 300 MHz): δ 1.35 (t, ^4J = 2.1 Hz, 2H, CH_{res}), 1.59 (dd, ^3J = 7.7 Hz, ^4J = 2.0 Hz, 2H, CH_{res}), 3.15 (t, ^3J = 4.9 Hz, 4H, CH_2O), 3.50 (t, ^3J = 4.9 Hz, 4H, CH_2O), 3.59−3.74 (m, 16H, CH_2O), 5.39 (dd, ^3J = 7.9 Hz, ^4J = 2.2 Hz, 2H, CH_{res}), 5.53 (t, ^3J = 8.0 Hz, 2H, CH_{res}), 7.78−7.86 (m, 12H, $CH_{Ph\ meta/para}$), 8.21−8.24 (m, 8H, $CH_{Ph\ ortho}$), 9.11 (s, 8H, $CH_{\beta\text{-pyrrolic}}$, $^4J_{Sn-H}$ = 12.4 Hz). ^{13}C NMR ($CDCl_3$, 75 MHz): δ 66.3 (CH_2O), 69.5 (CH_2O), 70.6 (2×CH_2O), 70.9 (CH_2O), 71.0 (CH_2O), 103.2 (CH), 103.6 (CH), 110.4 (CH), 121.8 (C_{quat}), 126.3 (CH), 127.0 (CH), 128.3 (CH), 132.6 (CH), 134.9 (CH), 141.0 (C_{quat}), 147.3 (C_{quat}). UV−vis (CH_2Cl_2) λ max (nm) (ε, mol^{-1} L cm^{-1}) 425 (2.7×10^5), 561 (1.6×10^4), 600 (0.9×10^4). Anal. Calcd. for $C_{68}H_{60}N_4O_9Sn \cdot H_2O$: C, 67.22; H, 5.11; N, 4.61. Found: C, 67.29; H, 5.19; N, 4.07. MALDI-TOF MS: m/z obsd 1197.32, calcd 1197.34 [(M+H)$^+$; M = $C_{68}H_{60}N_4O_9Sn$].

X-ray Crystallography. Data (Tables S1 and S2, see the Supporting Information) were collected on a Bruker SMART CCD diffractometer with Mo−Kα radiation. The structures were solved using SHELXS-97 and refined by full matrix least-squares on F^2 using SHELXL-97 with anisotropic thermal parameters for all non hydrogen atoms. The hydrogen atoms were introduced at calculated positions and not refined (riding model).

CCDC 755098−755104 contain the supplementary crystallographic data for compounds **3**−**4**, **6**, and **35**−**38**. These data can be obtained free of charge via www.ccdc.cam.ac.uk/data_request/cif.

Acknowledgment. Université de Strasbourg, International Centre for Frontier Research in Chemistry (FRC), Strasbourg, Institut Universitaire de France, the CNRS, and the Ministry of

Education and Research are acknowledged for financial support and for a scholarship to A.G. Dr. L. Allouche and J.-D. Sauer are acknowledged for performing the 2-D NMR experiments.

Supporting Information Available: Crystallographic data in CIF format, ^{1}H NMR Spectra of **35**−**36** in the presence of acids, ^{1}H NMR spectra and Roesy spectra of **1**−**2** in the presence of AgOTf, ^{1}H NMR spectra of **3**−**6** in the presence of AgOTf, and Tables of ^{1}H NMR chemical shifts for **1**−**6** in the presence of AgOTf. This material is available free of charge via the Internet at http://pubs.acs.org.